HHS Public Access

Author manuscript

Nat Neurosci. Author manuscript; available in PMC 2013 October 21.

Published in final edited form as:

Nat Neurosci. 2012 December ; 15(12): 1655–1666. doi:10.1038/nn.3259.

GKAP/SAPAP orchestrates activity-dependent postsynaptic protein remodeling and homeostatic scaling

Seung Min Shin[1], **Nanyan Zhang**[1], **Jonathan Hansen**[1], **Nashaat Z. Gerges**[2], **Daniel T.S. Pak**[3], **Morgan Sheng**[4,5], and **Sang H. Lee**[1,1]

[1]Department of Pharmacology and Toxicology, Medical College of Wisconsin, Milwaukee, Wisconsin, USA

[2]Department of Cell Biology and Neurobiology, Medical College of Wisconsin, Milwaukee, Wisconsin, USA

[3]Department of Pharmacology, Georgetown University Medical Center, Washington, District of Columbia, USA

[4]The Picower Institute for Learning and Memory, Massachusetts Institute of Technology, Cambridge, Massachusetts, USA

Abstract

How does chronic activity modulation lead to global remodeling of proteins at synapses and synaptic scaling? Here we report a role of guanylate-kinase-associated-protein (GKAP; also known as SAPAP), a scaffolding molecule linking NMDA receptor-PSD-95 to Shank-Homer complexes, in these processes. Over-excitation removes GKAP from synapses via ubiquitin-proteasome system, while inactivity induces synaptic accumulation of GKAP in rat hippocampal neurons. The bi-directional changes of synaptic GKAP levels are controlled by specific CaMKII isoforms coupled to different Ca^{2+} channels. α-CaMKII activated by NMDA receptor phosphorylates Serine-54 of GKAP to induce poly-ubiquitination of GKAP. In contrast, β-CaMKII activation via L-type voltage-dependent calcium channel promotes GKAP recruitment by phosphorylating Serine-340 and Serine-384 residues, which uncouples GKAP from MyoVa motor complex. Remarkably, overexpressing GKAP turnover mutants not only hampers activity-dependent remodeling of PSD-95 and Shank but also blocks bi-directional synaptic scaling. Therefore, activity-dependent turnover of PSD proteins orchestrated by GKAP is critical for homeostatic plasticity.

*Correspondence should be addressed to S.H.L (shlee@mcw.edu).

[5]present address: Department of Neuroscience, Genentech, Inc., 1 DNA Way, South San Francisco, California, USA.

Author Contributions: S.M.S, N.Z., J.H., and S.H.L. conducted all experiments and analyzed the data. N.Z.G., D.T.S.P., M.S., and S.H.L. contributed to designing experiments and interpretation of the data. S.H.L. and M.S. wrote the manuscript.

Supplementary Information: Supplementary information contains 13 Supplementary Figures.

Introduction

Synapses are continuously modified by usage and experience. This synaptic plasticity is believed to be a basis of information storage in the brain. Hebbian-type plasticity, such as long-term potentiation (LTP) and long-term depression (LTD), is relatively rapid, synapse-specific, and positive-feedback mechanisms. LTP and LTD are mediated mainly by the trafficking of AMPA receptors (AMPARs) into and out of stimulated synapses[1]. In contrast, homeostatic plasticity involves the global modification of synapses and operates over longer timescales. Homeostatic plasticity provides a global negative feedback and is crucial for stabilizing neuronal network function[2]. Synaptic scaling represents one form of homeostatic plasticity occurring at excitatory neurons, and adjusts the strength of all excitatory synapses up or down by modifying AMPAR levels[2]. Several molecules – e.g, BDNF, CaMKII, Arc, Plk2, TNF-α, all-*trans* retinoic acid, and mGluR-Homer1a – have been identified to be involved in synaptic scaling (reviewed in Refs. 2, 3). However, the detailed signaling pathways and molecular and biochemical changes at synapses associated with homeostatic synaptic scaling still need to be established[2, 3].

Activity-dependent protein turnover at the synapses by the ubiquitin-proteasome system (UPS) has emerged as a mechanism associated with the long-term global modification of synapses[4]. Interestingly, the activity-dependent changes in postsynaptic density (PSD) components occur in an ensemble fashion, with specific groups of PSD proteins accumulating or declining with similar kinetics and magnitudes. Such coordinated regulation could be explained if the UPS targets a few “master organizing” molecules in the PSD that are important for recruiting other PSD components[4]. The identity of these master organizing molecules is unknown, but good candidates are two scaffold proteins — GKAP and Shank family proteins — that are among the most highly poly-ubiquitinated proteins in the PSD[4]. The biochemical changes at synapses accompanied by chronic activity modulation, especially one regulated by the UPS, provide a potential molecular mechanism for homeostatic plasticity.

GKAP is a family of four scaffold proteins initially identified by their interaction with the guanylate kinase (GK) domain of PSD-95 (hence named, guanylate kinase associated protein, or SAPAP and DAP for SAP90/PSD-95-associated protein and hDLG-associated protein, respectively)[5-7]. In addition to PSD-95 family proteins, GKAP directly binds to other proteins including Shank[8] and 8-kDa dynein light chain (DLC)[9]. GKAP is one of the most abundant postsynaptic scaffolding proteins in the PSDs[10], and it has been shown to be essential for the recruitment/accumulation of Shank at excitatory synapses[11]. Therefore, synaptic GKAP protein level might contribute to synaptogenesis and dendritic spine morphogenesis by providing mutual reinforcement for the Shank-Homer complex[11, 12].

CaMKII is a multi-functional protein kinase, highly enriched in the PSDs, and serves a central role in synaptic plasticity, and learning and memory[13, 14]. *CaMKII* is encoded by four genes in mammals; α, β, γ, and δ. α- and β-CaMKII are predominant isoforms in the brain. They showed similar, broad substrate specificity in vitro[15]. However, accumulating evidence indicates CaMKII also have isoform-specific functions. α-CaMKII is critical for hippocampal LTP[14] and serves as a scaffold for the recruitment of proteasomes to dendritic

spines[16]. In contrast, β-CaMKII is important for neurite extension[17], for the maintenance of dendritic spine structure[18], for the dendritic patterning through centrosome regulation[19], and for the proper synaptic targeting of α-CaMKII[20]. They are also differentially regulated by activity [21-24]. Chronic elevated excitatory activity increased the α-CaMKII/β-CaMKII ratio, while inactivity decreased the α/β ratio. Furthermore, the general CaMKII inhibitor KN-93 or β-CaMKII knockdown prevented the changes in AMPA receptor (AMPAR) mEPSC by activity blockade[22, 23]. These results suggest that CaMKII is involved in the expression of synaptic scaling. However, the regulatory targets of α- and β-CaMKII isoforms mediating homeostatic plasticity remain unclear.

In this paper, we report that the bi-directional regulation of GKAP levels at synapses is controlled by differential phosphorylation of GKAP by different CaMKII isoforms, which are activated by Ca^{2+} entry through different channels. Furthermore, the turnover of GKAP at synapses is required for the normal activity-dependent remodeling of PSD protein composition, as well as homeostatic synaptic scaling.

Results

CaMKII controls activity-dependent GKAP turnover at synapses

Chronic activity modulation of cultured hippocampal neurons induces bi-directional and reversible changes in the protein composition of PSD[4]. GKAP was one of major scaffolding proteins that showed an activity-dependent turnover at PSDs [4]. Because CaMKII is regulated by activity and plays a role in the activity-dependent recruitment of proteasomes[16], we tested whether CaMKII is involved in the regulation of GKAP. Blocking CaMKII activity with KN-93, but not inactive analog KN92, abolished not only the tetrodotoxin (TTX)-dependent accumulation but also the bicuculline (Bic)-induced depletion of GKAP and PSD-95 from synaptic sites (Fig. 1a,b,d,e). KN-93 or KN-92 alone had no significant effects on the synaptic levels of GKAP and PSD-95 (Fig. 1c,d,e). Thus, CaMKII activity controls both activity-dependent accumulation and removal of GKAP and PSD-95 at synapses.

How does CaMKII activity regulate both recruitment/accumulation and removal of GKAP at synapses, seemingly opposed processes? Since CaMKII requires Ca^{2+} for activation, we addressed whether the sources of the Ca^{2+} influx are different, by blocking two major neuronal Ca^{2+} channels, NMDA receptors and L-type voltage-dependent Ca^{2+} channel (L-VDCC). Notably, the NMDA receptor antagonist AP5 completely abolished Bic-induced GKAP and PSD-95 removal but had no effect on TTX-dependent GKAP and PSD-95 accumulation at synapses (Fig. 1f,g). On the other hand, the L-VDCC antagonist nimodipine (Nimo), prevented the TTX-induced accumulation of GKAP and PSD-95 but had no effect on Bic-induced depletion of GKAP and PSD-95. Nimo alone did not affect the basal number of GKAP and PSD-95 puncta significantly. Thus, CaMKII activation through NMDA receptor promotes removal of GKAP and PSD-95 from synapses, whereas CaMKII activation mediated by L-VDCC increases the abundance of these proteins at synapses.

CaMKII isoform-specific regulation of GKAP turnover

To gain further insight into the molecular basis of CaMKII-dependent bi-directional control of GKAP, we analyzed the role of two specific CaMKII isoforms, α-CaMKII vs β-CaMKII, which are highly expressed in neurons. Plasmid-based RNA interference (RNAi) constructs expressing small hairpin RNAs were employed to suppress specifically α-CaMKII or β-CaMKII, whose specificity and efficacy were demonstrated in Supplementary Fig. 1a and previously[16, 18].

RNAi knockdown of α-CaMKII (α RNAi) did not affect synaptic levels of GKAP significantly under normal growth condition (Control) (Fig. 2a,b and Supplementary Fig. 1b,d), but completely blocked Bic-induced decrease in synaptic GKAP levels (Fig. 2a,b and Supplementary Fig. 1c,d). In contrast, α RNAi had no effect on the increase of GKAP level by TTX. Furthermore, overexpression of β-CaMKII with α RNAi did not restore the Bic-induced loss of synaptic GKAP (Supplementary Fig. 1b,c,d). These results indicate that α-CaMKII is specifically required for the Bic-stimulated removal of GKAP from synapses. Unlike α RNAi, RNAi knockdown of β-CaMKII (β RNAi) significantly reduced the number of GKAP clusters to less than 40% of control level under untreated control condition (Fig. 2a,b). This could reflect the requirement of β-CaMKII for GKAP accumulation in synapses, or might be secondary to the loss of dendritic spines, since β-CaMKII is implicated in synapse formation and the maintenance of dendritic spines[17, 18]. Nonetheless, β RNAi-transfected neurons still exhibited further reduction in the number of GKAP clusters ($P < 0.001$) after Bic treatment. However, β RNAi completely blocked the increase of GKAP cluster numbers stimulated by TTX (Fig. 2a,b). Thus, β-CaMKII is required for the increase of synaptic GKAP by TTX. To corroborate the finding, we co-expressed β RNAi and the actin-association domain of β-CaMKII (β285-542) which partly rescued the β RNAi-mediated loss of dendritic spines[18]. However, these neurons still failed to show TTX-induced increase of GKAP clusters (Fig. 2b). To test the role of actin-association in the differential function of CaMKII isoforms, we generated a chimeric α-CaMKII (designated α-CaMKII-AD) which has the actin association domain grafted from β-CaMKII (see diagram in Fig. 2c). When the α-CaMKII-AD was co-transfected in neurons with β RNAi, remarkably, it restored TTX-dependent increase of GKAP at synapses (Fig. 2c,d and Supplementary Fig. 1e). In contrast, co-expression of wildtype (WT) α-CaMKII failed to rescue the defects caused by β RNAi expression (Fig. 2d). Co-expression of RNAi-resistant versions of respective CaMKII isoforms with RNAi restored the activity-dependent turnover of GKAP to normal (Supplementary Fig. 1a,f). Thus, these data indicate that the synaptic accumulation of GKAP during inactivity requires β-CaMKII activity and the actin-association of β-CaMKII is critically important for the process.

We next examined the effect of Bic and TTX on the activation of the two CaMKII isoforms in hippocampal neurons. Bic increased the activation of both α- and β-CaMKII by > 6-fold compared to untreated control condition (Fig. 2e), which were determined by phospho-CaMKII antibody that recognizes autophosphorylation of both isoforms (pT286 and pT287 for α and β, respectively). In contrast, suppressing activity by TTX increased the autophosphorylation of β-CaMKII by > 3-fold after 12 h without significant changes in phospho-α-CaMKII levels (Fig. 2e,f). After 24 h TTX treatment, β-CaMKII again showed >

3-fold higher levels of autophosphorylation than α-CaMKII. Neither Bic nor TTX significantly changed the total amount of both CaMKII isoforms. These results indicate that β-CaMKII is a dominantly active form of CaMKII isoforms during chronic inactivity.

CaMKII activity promotes GKAP degradation by the UPS

We have shown that increasing activity removes GKAP from synapses (Fig. 1b,d,e), which is likely due to degradation of GKAP by the UPS[4]. As shown in Fig. 3a, Bic treatment (24 h) significantly decreased total GKAP protein level to ∼20% control. Incubation with proteasome inhibitors, MG132 or lactacystin (Lactacys) increased total GKAP level (> 180 %) similarly to TTX. Total GKAP level was increased to ∼150% of baseline by 24 h TTX, as well as AP5 or CNQX. In contrast, total GluR2/3 protein levels were not significantly affected by any of these treatments (Fig. 3a,c). Remarkably, co-incubation with KN-93, but not KN92, prevented the Bic-induced decrease of GKAP protein levels (Fig. 3b,c), indicating the involvement of CaMKII in GKAP degradation.

Although these data suggest that GKAP undergoes UPS-dependent degradation, it is unclear whether GKAP is directly ubiquitinated in a CaMKII regulated manner. To address this, we performed in vitro ubiquitination assays. When purified recombinant GST fusion protein of full-length GKAP was incubated with ubiquitin and P2 fraction (synaptosome enriched fraction) of rat forebrain as a source of E2/E3 enzymes (Fig. 3d), multiple GST-GKAP protein bands of higher molecular weights appeared (indicated by brackets) at the expense of normal size protein band (arrow line). The higher molecular weight shifts did not happen in the absence of Ca^{2+} ion (–lanes) and P2 fraction (–P2 lanes). More importantly, the molecular shifts were inhibited by the substitution of normal Ub for a triple lysine mutant of Ub (3KR-Ub), which cannot catalyze the poly-ubiquitination chain elongation. This result indicates that the higher molecular weight GKAP bands represent bona fide poly-ubiquitinated GKAP. Finally, blocking of CaMKII activity in the P2 fraction by KN93 completely abolished the poly-ubiquitination of GKAP. GST alone did not show such mobility shifts in any of these condition (data not shown). Collectively, these results indicate that GKAP undergoes poly-ubiquitination by brain synaptosome extracts in a manner dependent on the presence of Ca^{2+} and CaMKII activity.

We also examined by immunostaining the effect of proteasome inhibitors, MG132 and lactacystin, on Bic-induced removal of GKAP from synapses. Surprisingly, these proteasome inhibitors did not block the Bic-induced depletion of synaptic GKAP — the cluster density of GKAP was similarly reduced by Bic in the presence or absence of these proteasome inhibitors (Fig. 3e,f). Rather, GKAP formed large aggregates in the soma and proximal dendrites after treatment of neurons with Bic + MG132 or Bic + Lactacys (Fig. 3e, bottom panels), which is often seen for ubiquitinated proteins after the inhibition of proteasome activity[25]. In contrast, PSD-95 did not show such big aggregation after treatment with Bic and proteasome inhibitors. None of these treatments significantly affected the cluster density of PSD-93/Chapsyn-110. These results suggest that GKAP is degraded by proteasomes after being transported away from synapses, rather than being degraded directly at the synapse.

GKAP is a substrate of CaMKII

Is GKAP phosphorylated by CaMKII directly? To test this hypothesis, we first performed *in situ* phosphorylation assay of PSDs[26], in which purified PSDs were incubated with ^{32}P-ATP under conditions either promoting (by adding Ca^{2+} and CaM) or suppressing (by adding EGTA) endogenous CaMKII activity present in the PSD. Phosphorylation of GKAP, Shank, or NR2B was examined by subsequent immunoprecipitation (IP) of these proteins under denaturing condition to minimize co-precipitation of interacting proteins. As shown in Fig. 4a, addition of Ca^{2+}-CaM stimulated phosphorylation of multiple bands in the PSD fraction (lane 2). The stimulation of endogenous CaMKII activity strongly increased incorporation of ^{32}P-phosphate into GKAP and Shank, in addition to the known CaMKII substrate NR2B[26]. These data show that GKAP can be phosphorylated by CaMKII in the PSD.

To further determine whether CaMKII phosphorylates GKAP directly, we performed *in vitro* phosphorylation of purified GST-fusion proteins of various domains of GKAP using purified rat brain CaMKII (Fig. 4b; for domain structure of GKAP, see Fig. 4c). The repeat regions of GKAP which bind to PSD-95 (R1-R2, R1-R3, and R3-R5), as well as the DLC-binding domain of GKAP (DLC-BD), were directly phosphorylated by CaMKII in a Ca^{2+}/CaM-dependent manner. The GK domain of PSD-95 that binds to GKAP was not phosphorylated, showing the specificity of the reaction. These results suggest that GKAP is a substrate of CaMKII in the PSD.

CaMKII phosphorylation attenuates GKAP binding to PSD-95

Because the N-terminal repeat region of GKAP mediates direct interaction with PSD-95[5], we hypothesized that CaMKII phosphorylation of this region (see Fig. 4b) would disrupt the GKAP–PSD-95 interaction. GKAP and PSD-95 formed co-clusters when overexpressed together in COS cells[5] (cluster formation in 95% cells examined; see d1 in Fig. 4d). When expressed alone, they show diffuse staining without any cluster formation (data not shown). Formation of GKAP–PSD-95 co-clusters was almost completely prevented by the co-expression of constitutively active form of α-CaMKII (T286D mutant; cluster formation in only 8% cells); in these cells, distribution of GKAP and PSD-95 was largely diffuse (see d2 in Fig. 4d). Co-expression of wild-type (WT) α-CaMKII also inhibited co-clustering, though to a lesser extent than T286D mutant (cluster formation in 60% cells; d3 in Fig. 4d). In contrast, co-expression of kinase-dead mutant of α-CaMKII (K42R) had no effect on co-clustering (cluster formation in 95% cells; d4 in Fig. 4d), indicating that protein kinase activity of CaMKII is required for the disruption of the GKAP-PSD-95 complex. Thus, α-CaMKII activity can regulate the association of GKAP and PSD-95 in cells.

GKAP1/SAPAP1 contains multiple sequences that conform to the CaMKII phosphorylation consensus of (K/R)xx(S/T)Φ (where S/T is the phosphorylation site, and Φ represents a hydrophobic amino acid)[27]. Among them, Ser residues (S54 and S201) in the R1 and R5 (conserved in all GKAP isoforms; for amino acid sequences, see Fig. 4c) have been shown to be phosphorylated *in vivo* by mass spectrometry studies of the PSD[28]. We tested whether phosphorylation of S54 and S201 affects GKAP interaction with PSD-95, by changing these residues to either Ala or Asp individually or in combination. Binding to PSD-95 was measured in the yeast two-hybrid system, in which GKAP was used as “bait”. Single

mutations of S54, S83 (in R2), S114 (in R3), S148 (in R4), or S201 to Ala or Asp did not affect GKAP interaction with the GK domain of PSD-95 (Supplementary Fig. 2a,b). However, when both S54 and S201 sites were mutated to Ala (S54&S201A) or Asp (S54&S201D), GKAP interaction with PSD-95 GK domain was greatly diminished (Supplementary Fig. 2b). Double mutations of S54&S83 had no effect on PSD-95 interaction, further showing the specificity (Supplementary Fig. 2b). In contrast, none of these mutations affected GKAP interaction with DLC2. Furthermore, S54&S201D mutant failed to form co-clusters with PSD-95 in COS cells (cluster formation in < 1% cells; d5 in Fig. 4d). These results suggest that S54 and S201 residues play a critical role in GKAP interaction with PSD-95, and phosphorylation of these residues impairs PSD-95 binding.

This conclusion was further supported by co-IP experiments (Fig. 4e). The amount of S54&S201A and S54&S201D mutants co-precipitating with Myc-PSD-95 was greatly reduced, compared to WT GKAP (Fig. 4e). On the other hand, the amount of all three GKAP proteins co-precipitating with Myc-DLC2 was not significantly different. Thus, residues S54 and S201 in the repeat region of GKAP are critical for GKAP interaction with PSD-95.

Phosphorylation of S54 is critical for GKAP ubiquitination

To determine the critical CaMKII phosphorylation site(s) in GKAP that induces poly-ubiquitination, we tested various GKAP mutants for in vitro ubiquitination. Remarkably, S54A mutant did not show poly-ubiquitination regardless of the presence of Ca^{2+}(Fig. 5a). Deletion of the entire R1 that contains S54, designated ΔR1, also failed to show poly-ubiquitination. In contrast, the phospho-mimic S54D mutant showed strong poly-ubiquitination, even in the absence of Ca^{2+}(Fig. 5a). The poly-ubiquitination of S54D mutant was effectively blocked by the 3KR-Ub but was not affected by the presence of CaMKII inhibitors, KN-93 or autocamtide-2 related inhibitory peptide (AIP) (Fig. 5b). Therefore, the poly-ubiquitination of S54D mutant does not requires Ca^{2+} and CaMKII activity, indicating that phosphorylation of S54 is necessary and sufficient to induce poly-ubiquitination of GKAP. Phospho-mimic or -defective mutations in the DLC-BD (S340&384D and S340&384A mutants) showed normal Ca^{2+}-dependent poly-ubiquitination pattern (Fig. 5c), further demonstrating the specificity of S54D mutation for the poly-ubiquitination of GKAP.

To confirm that the phosphorylation of S54 is involved in the Bic-dependent poly-ubiquitination of GKAP in neurons, GKAP was immunoprecipitated under the denaturing condition and examined for the presence of phoshop-S54 (pS54) using an antibody that showed > 100-fold specificity toward pS54 peptide over the non-phosphorylated peptide (Supplementary Fig. 3a). As shown in Supplementary Fig. 3b, the anti-pS54 antibody showed multiple immunoreactive GKAP bands of higher molecular weights (resembling the pattern of poly-ubiquinated GKAP) only in samples immunoprecipitated from Bic-treated neurons (Bic alone and Bic + MG132), and not from samples treated with TTX, TTX + MG132, or MG132 alone. These results demonstrate that chronic Bic treatment promotes specific phosphorylation of S54 residue and the poly-ubiquitination of GKAP in hippocampal neurons. In addition, these results predicted that S54A mutant would show a

defect in Bic-induced decrease. Indeed, when transfected into neurons, S54A failed to show Bic-dependent reduction (Fig. 5d,e,f). On the other hand, S54A clearly demonstrated TTX-induced accumulation at synapses ($P < 0.001$). In contrast, transfected WT GKAP clearly showed normal activity-dependent turnover similar to endogenous GKAP. Collectively, these results highlight the importance of S54 phosphorylation in poly-ubiquitination and activity-dependent degradation of GKAP.

Myosin Va transports GKAP to synapses

To unravel the molecular mechanisms behind the stabilization/recruitment of GKAP during inactivity, we examined the importance of GKAP association with an actin-based motor protein MyoVa (MVa), which was proposed as a potential mechanism for the transport of GKAP to synapses[9]. To test this possibility, we first thought to address the importance of GKAP interaction with DLC, which provides a bridge to MVa. DLC forms a dimer and binds to various targets via two conserved amino sequences, (K/R)xTQT or GIQVD (see Supplementary Fig. 4a)[29]. Peptides based on the two sequences bind the same binding pocket in DLC and prevented DLC interactions[29]. To prevent DLC interaction with GKAP, we utilized a synthetic peptide that has a DLC-binding consensus KETQT sequence fused to the antennapedia peptide sequence (designated Antp-KETQT), which facilitates neuronal uptake of the peptide[30]. Incubation of neurons with Antp-KETQT peptide for 18 h greatly reduced GKAP puncta density to less than 25% of control level (Supplementary Fig. 4b,d). In contrast, the numbers of NR1 and synaptophysin puncta were not significantly affected by Antp-KETQT, indicating that synapse numbers were not changed. Control peptide (Antp-Kv1.4) did not affect the cluster numbers of all examined proteins. Importantly, both Antp peptides did not change total protein levels of GKAP, PSD-95 and GluR2 (Supplementary Fig. 4e), indicating that the reduction in GKAP cluster numbers was not due to the reduction of total GKAP protein levels. To further corroborate the data, we used a mutant GKAP that has a deletion in DLC-BD (designated ΔDLC-BD). As shown in Supplementary Fig. 4f, ΔDLC-BD mutant was largely confined within dendritic shaft, indicating that synaptic targeting of ΔDLC-BD mutant was severely impaired. Taken together, these results suggest DLC-interaction is required for the proper targeting of GKAP to synapses.

We next thought the role of MyoVa in GKAP transport to synapse by employing MVa-specific RNAi-mediated knockdown. As shown in Supplementary Fig. 5a, when tested in COS cells, MVa RNAi specifically reduced MVa levels but had effect on neither PSD-95 nor GKAP. When introduced into neurons, MVa RNAi reduced MVa staining intensities to > 50% in soma and > 85% in dendrites (Supplementary Fig. 5b,c), showing effective knockdown of endogenous MVa. When transfected into neurons, MVa RNAi significantly reduced the number of GKAP clusters (Fig. 6a,b), and increased GKAP staining in the soma (Supplementary Fig. 5d,e). More importantly, MVa knockdown completely abolished the TTX-induced increase of GKAP levels at synapses, while it showed no effect on Bic-dependent reduction of synaptic GKAP clusters (Fig. 6c,d). These results strongly suggest that GKAP is actively recruited to synapses via MyoVa motor proteins.

Since MyoVa-DLC interaction is important for GKAP transport to synapses, we next examined the role of CaMKII in this process. The DLC-BD of GKAP contained two

potential CaMKII phosphorylation sites (S340 and S384; Fig. 4c), which may regulate GKAP-DLC interaction. We tested this possibility by co-IP experiments after expressing the phospho-mimic (S340&384D) and phospho-defective GKAP mutants (S340&384A) with DLC in COS cells. As shown in Fig. 6e, both WT and S340&384A mutant showed good co-IP with DLC. In contrast, S340&384D and ΔDLC-BD mutant failed to coimmunoprecipitate with DLC, suggesting that CaMKII phosphorylation of S340 & S384 prevents the interaction of GKAP with DLC. Thus, in terms of DLC interaction, S340&384A and S340&384D are dissociation and association mutants, respectively. When S340&384A and S340&384D mutants were transfected into neurons, they showed severely impaired synaptic targeting, as shown by a large reduction in their synaptic cluster numbers under control condition (Fig. 6f,g; $P < 0.001$). The S340&384D mutant showed the greatest impairment ($P < 0.001$ compared to S340&384A). Most importantly, neither mutants show the TTX-driven increase in synaptic cluster numbers (Fig. 6f,g; $P > 0.23$). These data indicate that both DLC interaction and CaMKII phosphorylation of DLC binding region are required for the proper GKAP targeting to synapses and accumulation of GKAP during inactivity.

GKAP turnover is required for homeostatic synaptic scaling

To examine the importance of GKAP turnover in other synaptic protein turnover and homeostatic synaptic scaling, we tried to utilize a GKAP turnover mutant that is defective in the bi- directional changes. When transfected into neurons, ΔR1 mutant showed synaptic targeting similar to that of the transfected WT GKAP(see Fig. 7a,b and Supplementary Fig. 6a). Also, the total expression levels of ΔR1 were very similar to WT GKAP (data not shown). However, notably, neither Bic nor TTX treatment significantly changed the amount of the ΔR1 mutant at synapses (Fig. 7a,b). Therefore, ΔR1 is a mutant GKAP defective in both-directional activity-dependent turnover at synapses.

To address the significance of GKAP turnover in activity-dependent remodeling of PSD proteins, we overexpressed GKAP ΔR1 in hippocampal neurons and examined its effect on two key scaffold proteins in the PSD, PSD-95 and Shank. WT GKAP was used as control since it showed normal activity-dependent turnover (Fig. 7a,b). Neurons overexpressing WT GKAP showed Bic- and TTX-dependent changes in levels of PSD-95 and Shank at synapses, which were indistinguishable from neighboring non-transfected neurons (Fig. 7a,c,d and Supplementary Fig. 6b). In contrast, both Bic- and TTX-driven changes in synaptic PSD-95 and Shank were abolished in neurons expressing GKAP (ΔR1) mutant (Fig. 7a,c,d). In addition, GKAP (ΔR1) mutant also blocked the phosphorylation of S295 residues (pS-295) of PSD-95 (Fig. 7e,f), which was shown to be important for the synaptic accumulation of PSD-95 during inactivity[31]. Further corroborating the conclusion, overexpression of the degradation mutant, S54A, specifically blocked the Bic induced reduction in synaptic PSD-95 levels, whereas it did not affect TTX-induced increase of PSD-95 (Supplementary Fig. 6c,d). Furthermore, GKAP targeting mutants, S340&384A and S340&384D, impaired normal activity-dependent turnover of PSD-95 in both direction (Supplementary Fig. 6e,f). Therefore, these results indicate that GKAP turnover is critical for the activity-dependent turnover of PSD-95 and Shank at synapses.

We then examined activity-dependent changes of surface AMPA receptors. Chronic activity modulation led to bi-directional changes in surface expression of AMPA receptors, which are associated with synaptic scaling. Neurons over-expressing WT GKAP exhibited similar activity-dependent changes (Fig. 7g,h). On the other hand, overexpression of the ΔR1 mutant eliminated the activity-dependent changes in the surface expression of both GluA1 and GluA2 in both Bic- and TTX-treated neurons (Fig. 7g,h).

The importance of GKAP turnover in synaptic scaling was further examined by directly measuring miniature excitatory postsynaptic currents (mEPSCs) in cultured hippocampal neurons (Fig. 8). The amplitude of basal mEPSCs was unaffected by overexpression of either WT or ΔR1 GKAP, compared to untransfected neurons in the same culture (Fig. 8a,b). Treatment with TTX caused an increase in mEPSC amplitude in WT GKAP-transfected cells as well as untransfected cells (Fig. 8b; $P < 0.01$). Conversely, Bic treatment reduced mEPSC amplitude in both WT GKAP-transfected and non-transfected neurons (Fig. 8a,b; $P < 0.01$). Also, the cumulative frequency plots of mEPSC amplitudes from WT GKAP-transfected neurons show leftward shift with Bic and rightward shift with TTX (Fig. 8c), consistent with synaptic scaling ($P < 0.001$, Kolmogorov-Smirnov test). In sharp contrast, neurons expressing ΔR1 did not show either TTX- or Bic-induced changes in the average mEPSC amplitude (Fig. 8b) or shifts in mEPSC amplitude distribution (Fig. 8c). Thus overexpression of the ΔR1 GKAP mutant blocks synaptic scaling in response to both hyper- and hypo-activity, just as it blocks the normal turnover of PSD-95 and Shank in synapses and prevents the increase in surface AMPA receptors. We did not observe significant changes the frequency of mEPSCs under any of these conditions (Fig. 8d). Consistent with the data, S54A mutant also blocked the Bic-dependent down scaling of mEPSCs (Supplementary Fig. 6g), and S340&384A and S340&384D mutant failed to support TTX-induced up scaling (Supplementary Fig. 6h).

To further confirm the importance of GKAP in synaptic scaling, we designed shRNA sequences targeting GKAP. The specificity and efficacy of GKAP shRNAs are shown in Supplementary Fig. 7. GKAP knockdown by GKAP RNAi (#3-1) did not influence the amplitude of basal mEPSCs significantly. However, GKAP RNAi completely abolished the both-directional synaptic scaling, while untransfected neighboring neurons clearly showed activity-dependent synaptic scaling (Fig. 8e). Notably, GKAP RNAi greatly reduced the mEPSC frequency (Fig. 8f), suggesting that GKAP RNAi reduced the number of synapses. GKAP RNAi also abolished activity-dependent turnover of PSD-95 and Shank (Supplementary Fig. 7e-g). The immunostaining and electrophysiological data indicate that activity-dependent turnover of GKAP is critical for regulation of synaptic protein composition and homeostatic synaptic scaling.

Finally, we addressed the relative importance of GKAP turnover in synaptic scaling with respect to other known players in synaptic scaling. For this, we examined two proteins, Arc and Plk2 (also known as SNK), whose expression is induced by over-excitation[32-36]. Overexpression of ΔR1 affected picrotoxin (PTX)-induced expression of neither Arc (Supplementary Fig. 8a,b) nor Plk2 (Supplementary Fig. 8c,d), indicating that ΔR1 did not impair the signaling pathway(s) leading to the induction of these proteins. Considering that ΔR1 overexpression effectively blocked synaptic scaling (Fig. 8), these results suggested

that GKAP turnover is necessary for Arc and Plk2 to exert their effect on synaptic scaling. To further corroborate this notion, we examined the effect of ΔR1 on the Plk2-mediated removal/degradation of PSD-95 from synapses[36]. Overexpression of Plk2 removed PSD-95 from synapse in the proximal dendrites of transfected neurons (Supplementary Fig. 8e-g). Co-overexpression of GKAP WT did not have significant influence on the PSD-95 removal. In contrast, co-overexpression of ΔR1 abolished Plk2-mediated removal of PSD-95 and S54A mutant showed the same effect (Supplementary Fig. 8e-g). These results suggest that GKAP removal at synapses is prerequisite for Arc and Plk2 action and further support the importance of activity-dependent GKAP turnover in synaptic scaling.

Discussion

Activity modifies the protein composition of the PSD. Synaptic scaffolding proteins are particularly well-suited for the “driver's” role in PSD remodeling since their change can influence the levels of multiple interacting proteins. GKAP is a central member of the axis of major scaffolds in the PSD, consisting of PSD-95-GKAP-Shank[10, 37]. However, compared to PSD-95 and Shank, which play various roles in synaptic function including glutamate receptor trafficking, synapse formation, and spine morphogenesis[37, 38], little is known about the cell biology and function of GKAP. In this paper, we defined a critical role for GKAP in activity-dependent turnover of PSD-95 and Shank in the PSDs and in homeostatic synaptic scaling.

UPS-dependent protein degradation has emerged as an important theme underlying synaptic plasticity[4, 16, 39, 40]. A distinguished characteristic of activity-dependent turnover of PSD proteins is that groups of synaptic proteins are co-regulated, perhaps via control of master organizing proteins within the PSD[4]. Several characteristics of GKAP fit well for an organizer role within the PSD. First, GKAP is an indispensable central linker for the assembly of PSD-95-GKAP-Shank complexes at synapses[8], and PSD-95, GKAP and Shank are mutually dependent on each other for stable accumulation at synapses[12, 41]. Indeed, activity-dependent turnover of PSD-95 and Shank was dependent on the turnover of GKAP. Second, GKAP is one of the direct substrates of the UPS (see Fig. 4; also Ref. 4). Third, and most importantly, the synaptic accumulation of GKAP is controlled bi-directionally by synaptic activity. Interestingly, the level of activity is decoded by different Ca^{2+} channels. Ca^{2+} influx through NMDA receptor triggers poly-ubiquitination and degradation of GKAP. On the other hand, Ca^{2+} influx through L-VDCC is required for the synaptic accumulation of GKAP during inactivity. However, it is unlikely that GKAP turnover controls all PSD protein remodeling processes. A group of PSD proteins showed opposite changes to GKAP in response to altered activity: e.g., NR2A and α-CaMKII[4]. Furthermore, following GKAP turnover, synaptic scaling requires additional players like Plk2 to target other synaptic protein complexes for activity-dependent degradation by the UPS[33, 36].

The opposing functions of α and β-CaMKII in the bi-directional synaptic scaling have been well documented [22-24] but the specific regulatory targets of these enzymes have remained unclear. Our finding indicates that GKAP is the critical substrate of these CaMKII isoforms for the activity-dependent control of synaptic strength. How does the activation of α- versus β-CaMKII exert differential effects on GKAP turnover? Importantly, activity modulates

synaptic levels of α- and β-CaMKII, rendering α-CaMKII as a dominant species during over-excitation, while leaving β-CaMKII as a major kinase during low-level activity[21-24]. Therefore, we expect that Ca^{2+} influx through NMDA receptors during high activity preferentially acts through α-CaMKII, which translocates to the PSD during high activity, and recruits proteasomes to dendritic spines[16]. On the other hand, Ca^{2+} influx through L-VDCCs during low level activity (activated by spontaneous release of glutamate and miniature EPSPs)[42] preferentially stimulates β-CaMKII, which has higher sensitivity to Ca^{2+}/CaM[43], is associated with actin concentrated at the base of dendritic spine heads[44], where L-VDCCs protein are also localized[45].

What are the underlying molecular mechanisms for GKAP depletion and accumulation at synapses? Our results suggest a removal mechanism in which α-CaMKII phosphorylation in the N-terminal repeat region of GKAP disrupts GKAP interaction with PSD-95 and promotes UPS-dependent degradation (see Supplementary Fig. 9a). While dissociation from PSD-95 requires phosphorylation of S54 and S201, S54 phosphorylation was sufficient for poly-ubiquitination of GKAP. Notably, S54D mutant did not show Bic-induced reduction. This is probably due to the overexpression-induced dominant–negative effect of inhibiting poly-ubiquitination of S54D itself by saturating specific E3 ubiquitin ligase. GKAP is likely transported away from synapses before degradation by proteasomes, since preventing proteasome activity did not protect synaptic GKAP but rather produced large aggregates of GKAP in the soma. However, this view is different from the previous report proposing in situ degradation of GKAP at synapses[4]. In addition, the report showed a completely opposite activity-dependent regulation of PSD-95[4]. At present the bases of these discrepancies are unclear but differences in the density of hippocampal neurons and the concentration of proteasome inhibitors applied to culture might have contributed. It is also unclear from our data whether ubiquitination of GKAP occurs at or near synapses. Further studies are necessary to address these questions.

For the accumulation mechanism for GKAP, as depicted in Supplementary Fig. 9b, we propose that β-CaMKII phosphorylation of S340 and S384 in the DLC-binding domain of GKAP promotes the dissociation of GKAP from MVa-DLC2 motor protein complexes that transport GKAP to the base of the PSDs, and then the “unloaded” GKAP incorporates into the PSDs. For this, β-CaMKII association with the actin cytoskeleton was critical, presumably because it provides spatially favored position to regulate the interaction. A similar regulatory role of CaMKII was shown for MVa-mediated transport of GluR1 to synapses[46] and for Kif17-mediated transport of Mint1-NMDAR complex in spines[47].

It is remarkable that deletion of R1 in GKAP was sufficient to block the both-directional activity-dependent turnover of GKAP, which is different from S54A mutation that blocked only Bic-induced removal from synapses. One major difference between these two mutants is the CaMKII-dependent dissociability from PSD-95. The S54A mutant possesses S201 that allows α-CaMKII to prevent GKAP interaction with PSD-95 by phosphorylation, as suggested by the impaired PSD-95 interaction of S54&201D mutant (Fig. 4e,f). In contrast, unlike WT GKAP, ΔR1 mutant retained ΔR1–PSD-95 co-clusters even in the presence of constitutively active α-CaMKII in COS cells (Supplementary Fig. 10). Thus, it is likely that deletion of the R1 likely induces changes in the overall conformation of the GKAP repeat

region, so that the additional α-CaMKII regulation site in the R5 (S201) is masked, rendering GKAP resistant to α-CaMKII regulation of its interaction with PSD-95. These results suggest that the dissociation of GKAP from PSD-95 is required for the accumulation/recruitment of GKAP. Further studies are required to clarify how deletion of R1 prevents GKAP accumulation by inactivity. Furthermore, the CaMKII isoform-specific phosphorylation of GKAP at differential sites needs to be tested by additional biochemical experiments.

Intriguingly, the RNAi-mediated knockdown of GKAP not only prevented synaptic scaling measured by changes in mEPSC amplitude (Fig. 8e) but, unlike GKAP turnover mutant ΔR1, also had an additional effect of reducing mEPSC frequency. Since mEPSC frequency is mostly determined by the number of synapses, the data suggest that GKAP RNAi led to the loss of synapses. Thus, GKAP is not only important for the activity-dependent remodeling of synapses and synaptic scaling but also an essential scaffolding protein of the PSDs for the maintenance of excitatory synapses.

Bic is a $GABA_A$ receptor antagonist commonly used for inducing synaptic scaling, and indirectly enhances overall excitatory activity in neurons by reducing inhibitory inputs to excitatory neurons. Synaptic scaling is thought to occur in all synapses[2], since cumulative histogram show a shift of entire mEPSC amplitude distribution toward smaller values after Bic treatment (Fig. 8c). Consistent with this idea, cumulative distribution of GKAP cluster intensities revealed a similar shift after Bic treatment (Supplementary Fig. 11c), indicating that Bic reduced the amount of GKAP from most synapses (if not all). Therefore, Bic has a global effect and, unlike synapse-specific Hebbian-type plasticity, synaptic scaling affects all synapses.

GKAP was shown to be poly-ubiquitinated by TRIM3 ubiquitin ligase[48], which raises a possibility that TRIM3 may involves in the CaMKII-mediated GKAP degradation. However, we were not able to observe a specific association of TRMI3 with pS54 peptide or S54D mutant by pull-down assays (data not shown), indicating that TRIM is unlikely involved in the CaMKII-dependent degradation of GKAP described here. CDK5 is another protein kinase involved in the GKAP degradation induced by soluble amyloid β[49]. However, this also likely represents an independent GKAP regulatory mechanism, since the CDK5 phosphorylation sites in GKAP are different from the α-CaMKII sites, and more importantly, CaMKII inhibitors did not prevent GKAP degradation by soluble amyloid β[49].

Finally, recent studies on knockout mice lacking SAPAP-3, a GKAP family member highly expressed in the striatum, showed unexpected behavioral abnormalities similar to obsessive-compulsive disorder[50]. Our findings on the critical role of GKAP/SAPAP in synapse remodeling and homeostatic plasticity offer potentially new ways to think about the pathophysiology of this condition.

Online Methods

Expression Constructs and shRNA plasmids

HA-GKAP was constructed by sub-cloning EcoR1 fragment of GKAP cDNA comprising the whole coding region into pGW1-HA. GKAP ΔR1 was generated by deleting SmaI-NcoI fragment from the HA-GKAP/pGW1. For electrophysiological experiments, GKAP or GKAP ΔR1 were sub-cloned into pIRES2-EGFP (Invitrogen). CaMKII RNAi constructs were based on pSuper plasmid as described before[18]. MyoVa and GKAP RNAi constructs were prepared by cloning the following nucleotide sequences (not including linker and loop sequences) into pSuper: GTAGAACGTCTTCAGCTAA (MyoVa), CAGTGGCAGCTACATCAAA (GKAP#1-1), and GGCAGCTACATCAAAGCCA (GKAP#3-1). GST-GKAP fusion protein expression vectors contained a flexible linker (SGGGGSASGGGGS) between GST and GKAP cDNA sequence to avoid steric hindrance that might hamper CaMKII phosphorylation of S54 of GKAP. α-CaMKII-AD construct was prepared by inserting a.a. 319-Gln-388-Val sequence of β-CaMKII into α-CaMKII residues between 322-Lys and 323-Lys.

Hippocampal Culture, Transfection, Antibodies, and Immunocytochemistry

Dissociated hippocampal neuron culture was prepared as described previously and grown in Neurobasal media supplemented with B27. All animal protocols were approved by the Medical College of Wisconsin Institutional Animal Care and Use Committee. Neurons were transfected at 14-15 DIV with Lipofectamine 2000 reagent. Neurons were fixed with cold methanol (-20 ºC) for staining of PSD-95, Shank, and GKAP. Alternatively, they were incubated first in 2% formaldehyde/4% sucrose/1 × PBS for 2 min followed by cold methanol for 10 min, for co-staining with β-Gal (or GFP) and CaMKII, GKAP, or PSD-95. For surface staining of GluA, neurons were fixed in 4% formaldehyde for 6 min, which is suboptimal for GKAP staining. GKAP antibodies used in the immunofluorescent staining, rabbit anti- GKAP (1:100)[5] or mouse anti-pan SAPAP (NeuroMab, 1:250), recognize all GKAP isoforms (data not shown). Other primary antibodies and their dilution used for immunocytochemistry are: mouse anti-β-Gal (Promega, 1:1,000), rabbit anti-β-Gal (abcam, 1:5,000), mouse anti-α-CaMKII (Zymed, 1:250), mouse anti-β-CaMKII (Zymed, 1:250), mouse anti-PSD-95 (K28/43 clone, Chemicon, 1:500), rabbit anti-pS295 PSD-95 (Abcam, 1:300), mouse anti-PSD-93/Chapsyn-110 (N18/30, NeuroMab; 1:100), rabbit anti-Shank (3856 antibody)[51], mouse anti-Bassoon (Stressgen, 1:200), mouse anti-synaptophysin (SVP-38, Sigma, 1:1,000), rabbit anti-HA (Santa Cruz, 1:100), mouse anti-HA (12CA5, Roche, 1:400), mouse anti-myc (9E10, Santa Cruz, 1:100), rabbit anti-Arc (Santa Cruz Biotechnology, 1:100), rabbit anti-SNK (Santa Cruz Biotechnology, 1:100), rabbit anti-GluR1 (Oncogene, 5 μg/ml), and mouse anti-GluR2 (Chemicon, 5 μg/ml). Bound primary antibodies were visualized by Alexa 488- (1:250) or Cy3-conjugated (1:500) secondary antibodies. Anti-phospho-S54 antibody was prepared by immunizing rabbits with KLH conjugated peptide (CRRMRSGpSYIKA) and purified by affinity chromatography using the antigen peptide after passing through non-phospho peptide column. Rabbit anti-phospho CaMKII antibody (Phospho solutions) and mouse anti-ubiquitin, K48-specific antibody (Millipore) were used for western blotting at 1:1,000 and 1:2,000 dilution, respectively.

Image Acquisition and Analyses

Images were captured by using Nikon C1 plus laser scanning confocal microscope. Acquired images (z-series stacks) were first converted to projection images (with maximal projection option) and analyzed using Metamorph software (Molecular Devices). To measure puncta number per given length of dendrites, per image, 5 dendritic segments (~15-30 μm in length each) were selected from transfected and neighboring non-transfected neurons, respectively. After applying threshold, only puncta with more than 3 pixel sizes were counted and their pixel area and total and average intensity were also measured. For quantification of HA-GKAP staining, clusters formed inside dendritic shafts were excluded from quantification to avoid erroneous inclusion of non-synaptic clusters. All data collected were transferred to Microsoft Excel for computation and statistical significance analyses. Image acquisition and analyses were done in a double-blind manner to eliminate experimenter bias,

Statistical Analysis

All values represent means ± s.e.m., unless otherwise indicated. All transfection experiments were done in a triplicate set. Statistical significance for pair was analyzed by the Student's *t* test (unpaired, two tailed, assuming unequal variance), unless otherwise indicated. ANOVA with Tukey's *post hoc* test were used for group comparisons. Cumulative plot data were analyzed by Kolmogrov-Smirnov test (K-S test). $P < 0.05$ was considered significant.

In situ and in vitro phosphorylation

In situ phosphorylation reaction was performed by incubating purified PSD I fraction (30 μg) at 37 ºC for 5 min in the 100 μl reaction mixtures of 20 mM HEPES (pH7.5), 10 mM Mg·acetate, 1 mM $CaCl_2$, 5 μM CaM, 0.5 μM ^{32}P-γ-ATP, 10 mM DTT, 0.1% Triton X-100, 1 μM microcystin-LR, 1 × protease inhibitor cocktail (Roche). Ca^{2+}–dependence was examined by substituting 1 mM EGTA for $CaCl_2$ and CaM in the reaction mixture. The reaction was immediately stopped by adding EDTA to final 25 mM and putting on ice. Phosphorylation of specific proteins was examined by subsequent immunoprecipitation with respective antibodies under denaturing condition[26]. Briefly, 1/10 vol. of 2% SDS (final 0.2% conc.) were added to the reaction mixture and boiled for 3 min. After centrifugation at 15,000 ×,*g* for 10 min at 4 ºC, supernatant were mixed with equal vol. of 2 × RIPA (20 mM Tris·Cl, pH7.4, 2 mM EDTA, 300 mM NaCl, 2% Triton X-100, 1% sodium deoxycholate, 1 mg/ml BSA). Aliquots were mixed with 5 μg of indicated antibodies and mixed overnight at 4 ºC, followed by protein-A sepharose beads (20 μl) incubation for additional 2 h. After washing the beads with 1×RIPA for 3 times, immunoprecipitated proteins were eluted by boiling in SDS sample buffer, followed by subsequent SDS-PAGE and autoradiography.

Coimmunoprecipitation

Coimmunoprecipitation of GKAP and PSD-95 or DLC was done as described before[9]. Briefly, HA-tagged GKAP constructs were co-transfected with either myc-tagged PSD-95 or myc-tagged DLC2 in COS cells using lipofectamine (Invitrogen). After 48 h post-transfection, harvested cells were lyzed in buffer A [50 mM Tris·Cl, pH7.4, 75 mM NaCl, 2.5 mM EDTA, 2.5 mM EGTA, 2 mM DTT, 1% SDS, protease inhibitor cocktail (Roche)].

After mixing by pipetting up-down briefly, the lysate was quickly quenched by 4× volume of buffer B (50 mM Tris·Cl, pH7.4, 150 mM NaCl, 2.5 mM EDTA, 2.5 mM EGTA, 2 mM DTT, 1% Triton X-100, protease inhibitor cocktail). After removing particulate materials by centrifugation at 16,000 × *g* for 30 min at 20 ºC, supernatant was used for immunoprecipitation using myc-agarose beads (Santa Cruz). For immunoprecipitation from brain tissues, GKAP was immunoisolated under the denaturing condition as described above.

In vitro Ubiquitination

Recombinant GST-GKAP protein was purified from bacteria using glutathione-Sepharose. Purified GST-GKAP (200 ng) was mixed with 4 μg of P2 membrane fraction in 15 μl reactions containing 50 mM Tris·Cl, pH7.6, 5 mM $MgCl_2$, ATP regenerating system (2 mM ATP, 10 mM creatine phosphate, 3.5 U/ml creatine kinase), 10 μg Ub, 10 ng E1, 2 μM Ub aldehyde, 0.1 mM $CaCl_2$, (or substituted by 2 mM EGTA), 1 μM microcystin. The reaction mixture was incubated at 37 ºC for 1 h, and immediately stopped by adding SDS sample buffer followed by boiling for 5 min. Proteins were separated on 6% SDS-polyacrylamide gels and ubiquitinated GKAP was examined by western blotting with anti-GST or anti-GKAP antibody.

Electrophysiology and mEPSC analysis

Hippocampal neurons, plated at the density of 150 kcells/coverslip, were transfected at 10 DIV with pIRES2-EGFP plasmid expressing either WT GKAP or ΔR1. After 1 d post-transfection, neurons were treated by either TTX (2 μM) or Bic (40 μM) for 48 h before recording. Transfected pyramidal neurons were identified by GFP fluorescence and morphological inspection. Whole cell patch recordings were performed by voltage-clamping neurons at –70 mV in bathing solution (in mM, 119 NaCl, 5 KCl, 2 $CaCl_2$, 2 $MgCl_2$, 30 glucose, 10 HEPES, pH7.4, 300 mOsm) containing TTX (1 μM) and Bic (20 μM), continuously perfused at the rate of ∼0.5 ml/min. Internal solution was composed of 140 K·gluconate, 5 KCl, 2 $MgCl_2$, 4 Mg·ATP, 0.3 Na_2·GTP, 0.2 EGTA, 10 HEPES and adjusted to pH7.2 and 290 mOsm. mEPSCs were acquired through a MultiClamp 700B amplifier (Molecular Devices), filtered at 2 kHz, digitized at 10 kHz, utilizing the “gap-free” protocol. mEPSCs were detected and analyzed with MiniAnalyses software (Synaptosoft) by setting amplitude threshold to 5 pA (usually √RMS × 3 values were lower than 4), further filtered by selecting mini events of 10-90% rise time < 3 msec. Cumulative probability plots were generated by combining mini events from all recorded neurons.

Supplementary Material

Refer to Web version on PubMed Central for supplementary material.

Acknowledgments

We thank Dr. Qing-song Liu for technical advice on electrophysiology. We appreciate Drs. Atsushi Tamada and Hiroyuki Kamiguchi (RIKEN Brain Science Institute) for providing MyoV expression vectors. This work was supported by US National Institutes of Health grant R01 MH078135 and Whitehall Foundation grant to S.H.L, and by US National Institutes of Health grant R01 AG032320 to N.Z.G.

References

1. Collingridge GL, Isaac JT, Wang YT. Receptor trafficking and synaptic plasticity. Nat Rev Neurosci. 2004; 5:952–962. [PubMed: 15550950]
2. Turrigiano GG. The self-tuning neuron: synaptic scaling of excitatory synapses. Cell. 2008; 135:422–435. [PubMed: 18984155]
3. Pozo K, Goda Y. Unraveling mechanisms of homeostatic synaptic plasticity. Neuron. 2010; 66:337–351. [PubMed: 20471348]
4. Ehlers MD. Activity level controls postsynaptic composition and signaling via the ubiquitin-proteasome system. Nat Neurosci. 2003; 6:231–242. [PubMed: 12577062]
5. Kim E, et al. GKAP, a novel synaptic protein that interacts with the guanylate kinase-like domain of the PSD-95/SAP90 family of channel clustering molecules. J Cell Biol. 1997; 136:669–678. [PubMed: 9024696]
6. Takeuchi M, et al. SAPAPs. A family of PSD-95/SAP90-associated proteins localized at postsynaptic density. J Biol Chem. 1997; 272:11943–11951. [PubMed: 9115257]
7. Satoh K, et al. DAP-1, a novel protein that interacts with the guanylate kinase-like domains of hDLG and PSD-95. Genes Cells. 1997; 2:415–424. [PubMed: 9286858]
8. Naisbitt S, et al. Shank, a novel family of postsynaptic density proteins that binds to the NMDA receptor/PSD-95/GKAP complex and cortactin. Neuron. 1999; 23:569–582. [PubMed: 10433268]
9. Naisbitt S, et al. Interaction of the postsynaptic density-95/guanylate kinase domain-associated protein complex with a light chain of myosin-V and dynein. J Neurosci. 2000; 20:4524–4534. [PubMed: 10844022]
10. Sheng M, Hoogenraad CC. The postsynaptic architecture of excitatory synapses: a more quantitative view. Annu Rev Biochem. 2007; 76:823–847. [PubMed: 17243894]
11. Sala C, et al. Regulation of dendritic spine morphology and synaptic function by Shank and Homer. Neuron. 2001; 31:115–130. [PubMed: 11498055]
12. Romorini S, et al. A functional role of postsynaptic density-95-guanylate kinase-associated protein complex in regulating Shank assembly and stability to synapses. J Neurosci. 2004; 24:9391–9404. [PubMed: 15496675]
13. Hudmon A, Schulman H. Neuronal CA2+/calmodulin-dependent protein kinase II: the role of structure and autoregulation in cellular function. Annu Rev Biochem. 2002; 71:473–510. [PubMed: 12045104]
14. Lisman J, Yasuda R, Raghavachari S. Mechanisms of CaMKII action in long-term potentiation. Nat Rev Neurosci. 2012; 13:169–182. [PubMed: 22334212]
15. Braun AP, Schulman H. The multifunctional calcium/calmodulin-dependent protein kinase: from form to function. Annu Rev Physiol. 1995; 57:417–445. [PubMed: 7778873]
16. Bingol B, et al. Autophosphorylated CaMKIIalpha acts as a scaffold to recruit proteasomes to dendritic spines. Cell. 2010; 140:567–578. [PubMed: 20178748]
17. Fink CC, et al. Selective regulation of neurite extension and synapse formation by the beta but not the alpha isoform of CaMKII. Neuron. 2003; 39:283–297. [PubMed: 12873385]
18. Okamoto K, Narayanan R, Lee SH, Murata K, Hayashi Y. The role of CaMKII as an F-actin-bundling protein crucial for maintenance of dendritic spine structure. Proc Natl Acad Sci USA. 2007; 104:6418–6423. [PubMed: 17404223]
19. Puram SV, et al. A CaMKIIbeta signaling pathway at the centrosome regulates dendrite patterning in the brain. Nat Neurosci. 2011; 14:973–983. [PubMed: 21725312]
20. Borgesius NZ, et al. betaCaMKII plays a nonenzymatic role in hippocampal synaptic plasticity and learning by targeting alphaCaMKII to synapses. J Neurosci. 2011; 31:10141–10148. [PubMed: 21752990]
21. Thiagarajan TC, Lindskog M, Malgaroli A, Tsien RW. LTP and adaptation to inactivity: overlapping mechanisms and implications for metaplasticity. Neuropharmacology. 2007; 52:156–175. [PubMed: 16949624]

22. Thiagarajan TC, Piedras-Renteria ES, Tsien RW. alpha- and betaCaMKII. Inverse regulation by neuronal activity and opposing effects on synaptic strength. Neuron. 2002; 36:1103–1114. [PubMed: 12495625]
23. Groth RD, Lindskog M, Thiagarajan TC, Li L, Tsien RW. Beta Ca2+/CaM-dependent kinase type II triggers upregulation of GluA1 to coordinate adaptation to synaptic inactivity in hippocampal neurons. Proc Natl Acad Sci USA. 2011; 108:828–833. [PubMed: 21187407]
24. Thiagarajan TC, Lindskog M, Tsien RW. Adaptation to synaptic inactivity in hippocampal neurons. Neuron. 2005; 47:725–737. [PubMed: 16129401]
25. Kopito RR. Aggresomes, inclusion bodies and protein aggregation. Trends Cell Biol. 2000; 10:524–530. [PubMed: 11121744]
26. Omkumar RV, Kiely MJ, Rosenstein AJ, Min KT, Kennedy MB. Identification of a phosphorylation site for calcium/calmodulindependent protein kinase II in the NR2B subunit of the N-methyl-D-aspartate receptor. J Biol Chem. 1996; 271:31670–31678. [PubMed: 8940188]
27. Songyang Z, et al. A structural basis for substrate specificities of protein Ser/Thr kinases: primary sequence preference of casein kinases I and II, NIMA, phosphorylase kinase, calmodulin-dependent kinase II, CDK5, and Erk1. Mol Cell Biol. 1996; 16:6486–6493. [PubMed: 8887677]
28. Trinidad JC, Thalhammer A, Specht CG, Schoepfer R, Burlingame AL. Phosphorylation state of postsynaptic density proteins. J Neurochem. 2005; 92:1306–1316. [PubMed: 15748150]
29. Lo KW, et al. The 8-kDa dynein light chain binds to p53-binding protein 1 and mediates DNA damage-induced p53 nuclear accumulation. J Biol Chem. 2005; 280:8172–8179. [PubMed: 15611139]
30. Passafaro M, Sala C, Niethammer M, Sheng M. Microtubule binding by CRIPT and its potential role in the synaptic clustering of PSD-95. Nat Neurosci. 1999; 2:1063–1069. [PubMed: 10570482]
31. Kim MJ, et al. Synaptic accumulation of PSD-95 and synaptic function regulated by phosphorylation of serine-295 of PSD-95. Neuron. 2007; 56:488–502. [PubMed: 17988632]
32. Beique JC, Na Y, Kuhl D, Worley PF, Huganir RL. Arc-dependent synapse-specific homeostatic plasticity. Proc Natl Acad Sci USA. 2011; 108:816–821. [PubMed: 21187403]
33. Seeburg DP, Feliu-Mojer M, Gaiottino J, Pak DT, Sheng M. Critical role of CDK5 and Polo-like kinase 2 in homeostatic synaptic plasticity during elevated activity. Neuron. 2008; 58:571–583. [PubMed: 18498738]
34. Evers DM, et al. Plk2 attachment to NSF induces homeostatic removal of GluA2 during chronic overexcitation. Nat Neurosci. 2010; 13:1199–1207. [PubMed: 20802490]
35. Shepherd JD, et al. Arc/Arg3.1 mediates homeostatic synaptic scaling of AMPA receptors. Neuron. 2006; 52:475–484. [PubMed: 17088213]
36. Pak DT, Sheng M. Targeted protein degradation and synapse remodeling by an inducible protein kinase. Science. 2003; 302:1368–1373. [PubMed: 14576440]
37. Sheng M, Kim E. The Postsynaptic Organization of Synapses. Cold Spring Harb Perspect Biol. 2011
38. Funke L, Dakoji S, Bredt DS. Membrane-associated guanylate kinases regulate adhesion and plasticity at cell junctions. Annu Rev Biochem. 2005; 74:219–245. [PubMed: 15952887]
39. Bingol B, Sheng M. Deconstruction for reconstruction: the role of proteolysis in neural plasticity and disease. Neuron. 2011; 69:22–32. [PubMed: 21220096]
40. DiAntonio A, Hicke L. Ubiquitin-dependent regulation of the synapse. Annu Rev Neurosci. 2004; 27:223–246. [PubMed: 15217332]
41. Kuriu T, Inoue A, Bito H, Sobue K, Okabe S. Differential control of postsynaptic density scaffolds via actin-dependent and -independent mechanisms. J Neurosci. 2006; 26:7693–7706. [PubMed: 16855097]
42. Sutton MA, et al. Miniature neurotransmission stabilizes synaptic function via tonic suppression of local dendritic protein synthesis. Cell. 2006; 125:785–799. [PubMed: 16713568]
43. Brocke L, Chiang LW, Wagner PD, Schulman H. Functional implications of the subunit composition of neuronal CaM kinase II. J Biol Chem. 1999; 274:22713–22722. [PubMed: 10428854]

44. Honkura N, Matsuzaki M, Noguchi J, Ellis-Davies GC, Kasai H. The subspine organization of actin fibers regulates the structure and plasticity of dendritic spines. Neuron. 2008; 57:719–729. [PubMed: 18341992]

45. Tippens AL, et al. Ultrastructural evidence for pre- and postsynaptic localization of Cav1.2 L-type Ca2+ channels in the rat hippocampus. J Comp Neurol. 2008; 506:569–583. [PubMed: 18067152]

46. Correia SS, et al. Motor protein-dependent transport of AMPA receptors into spines during long-term potentiation. Nat Neurosci. 2008; 11:457–466. [PubMed: 18311135]

47. Guillaud L, Wong R, Hirokawa N. Disruption of KIF17-Mint1 interaction by CaMKII-dependent phosphorylation: a molecular model of kinesin-cargo release. Nat Cell Biol. 2008; 10:19–29. [PubMed: 18066053]

48. Hung AY, Sung CC, Brito IL, Sheng M. Degradation of postsynaptic scaffold GKAP and regulation of dendritic spine morphology by the TRIM3 ubiquitin ligase in rat hippocampal neurons. PLoS One. 2010; 5:e9842. [PubMed: 20352094]

49. Roselli F, Livrea P, Almeida OF. CDK5 Is Essential for Soluble Amyloid beta-Induced Degradation of GKAP and Remodeling of the Synaptic Actin Cytoskeleton. PLoS One. 2011; 6:e23097. [PubMed: 21829588]

50. Welch JM, et al. Cortico-striatal synaptic defects and OCD-like behaviours in Sapap3-mutant mice. Nature. 2007; 448:894–900. [PubMed: 17713528]

51. Lim S, et al. Characterization of the Shank family of synaptic proteins. Multiple genes, alternative splicing, and differential expression in brain and development. J Biol Chem. 1999; 274:29510–29518. [PubMed: 10506216]

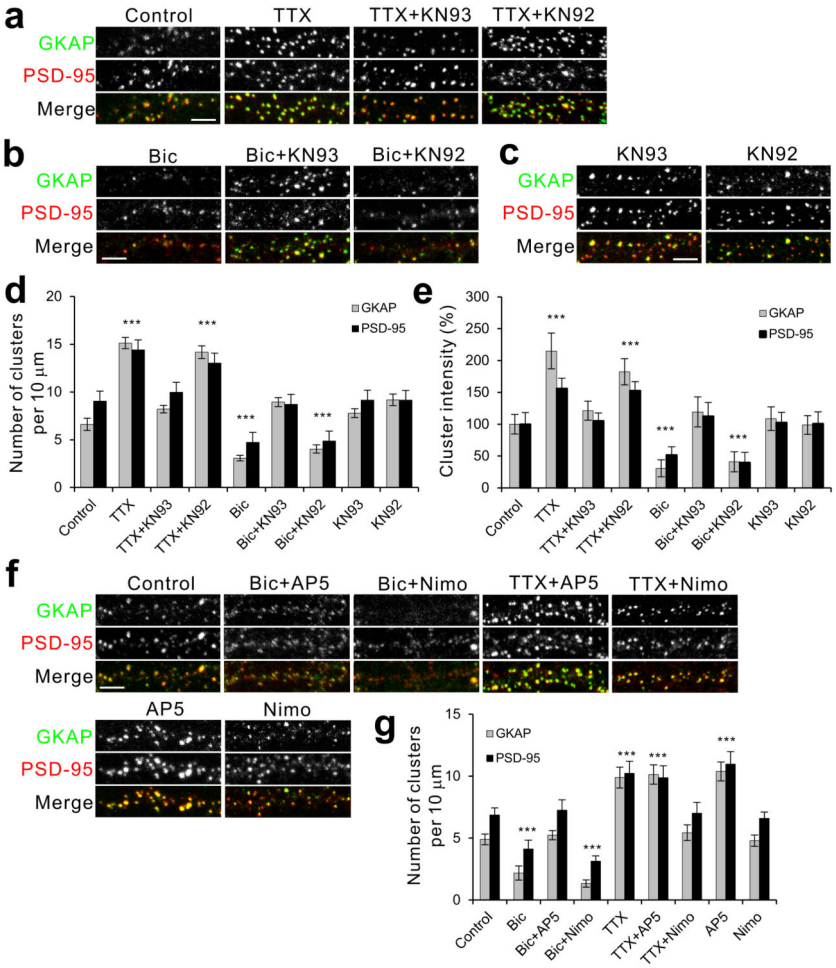

Figure 1.

CaMKII activity is required for both Bic-induced removal and TTX-dependent accumulation of GKAP and PSD-95 at synapses.

(**a,b**) Changes in the GKAP and PSD-95 clusters 24 h after treatment with either (**a**) TTX (2 µM) alone, TTX + KN-93 (10 µM), or TTX + KN-92 (10 µM), or (**b**) Bic (40 µM) alone, Bic + KN-93 (10 µM), or Bic + KN-92 (10 µM). (**c**) Effect of KN-93 or KN-92 alone on GKAP and PSD-95 clusters.

(**d,e**) Quantification of GKAP and PSD-95 cluster density (**d**) and intensities (**e**) 24 h after the indicated treatments. Each bar represents mean ± s.e.m. $n \geq 20$ neurons per condition.***$P < 0.001$ compared to Control. (**f**) Effect of AP5 (100 µM) and Nimo (5 µM) on Bic- or TTX-induced changes of GKAP and PSD-95 clusters at synapses. (**g**) Quantitative analysis shows effect of the Ca^{2+} channel blockers on the density of GKAP and PSD-95 clusters. Each bar represents mean ± s.e.m. $n \geq 20$ neurons per condition.

*** $P < 0.001$. Scale bars, 5 µm.

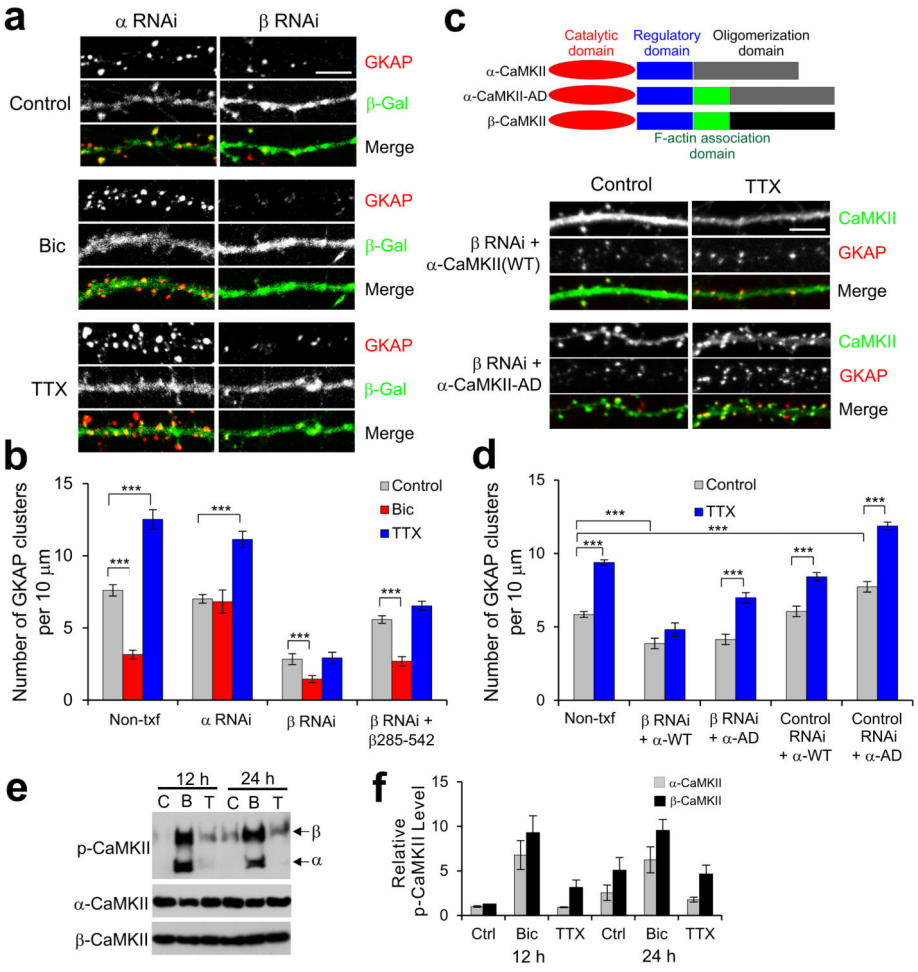

Figure 2.

CaMKII isoform-specific regulation of activity-dependent GKAP turnover. (**a**) Effect of isoform-specific CaMKII RNAi on activity-dependent turnover of endogenous GKAP. Cultured hippocampal culture neurons (14 DIV) were transfected with α RNAi + β-galactosidase (β-Gal) or β RNAi + β-Gal. After 1 d post-transfection, neurons were treated with either Bic (40 μM) or TTX (2 μM) for 24 h and examined for the changes in GKAP clusters (red) by immuno-fluorescence staining. Transfected neurons were identified by β-Gal immunofluorescence (green). (**b**) Quantification of CaMKII RNAi effect on activity-dependent turnover of endogenous GKAP, measured by the changes in the cluster density from non-transfected neighboring neurons (Non-txf) and RNAi-transfected neurons. $n > 20$ per each construct. *** $P < 0.001$. (**c**) Rescue of β RNAi by a chimeric α-CaMKII with actin association domain of β-CaMKII (α-CaMKII-AD). Hippocampal neurons were transfected with β RNAi + α-CaMKII (WT) or β RNAi + α-CaMKII-AD, treated with TTX for 24 h, and immunostained for the CaMKII (green) and GKAP (red). Schematic diagram of CaMKII constructs are shown above the representative images. (**d**) Quantification of β RNAi rescue by α-CaMKII-AD on GKAP cluster density. $n > 20$ per each construct. *** $P < 0.001$. (**e**) Activation of CaMKII isoforms in Bic or TTX-treated hippocampal neurons. Neurons were untreated (C) or treated with Bic (B; 40 μM) or TTX (T; 2 μM) for 12 or 24 h.

Total protein extracts were examined for protein levels of autophosphorylated-CaMKII (p-CaMKII) or individual CaMKII isoform. Full-length blots are presented in Supplementary Figure 13. Quantification of relative phospho-α-CaMKII and phospho-β-CaMKII levels (n = 3). Scale bars, 5 μm. Error bars represent s.e.m.

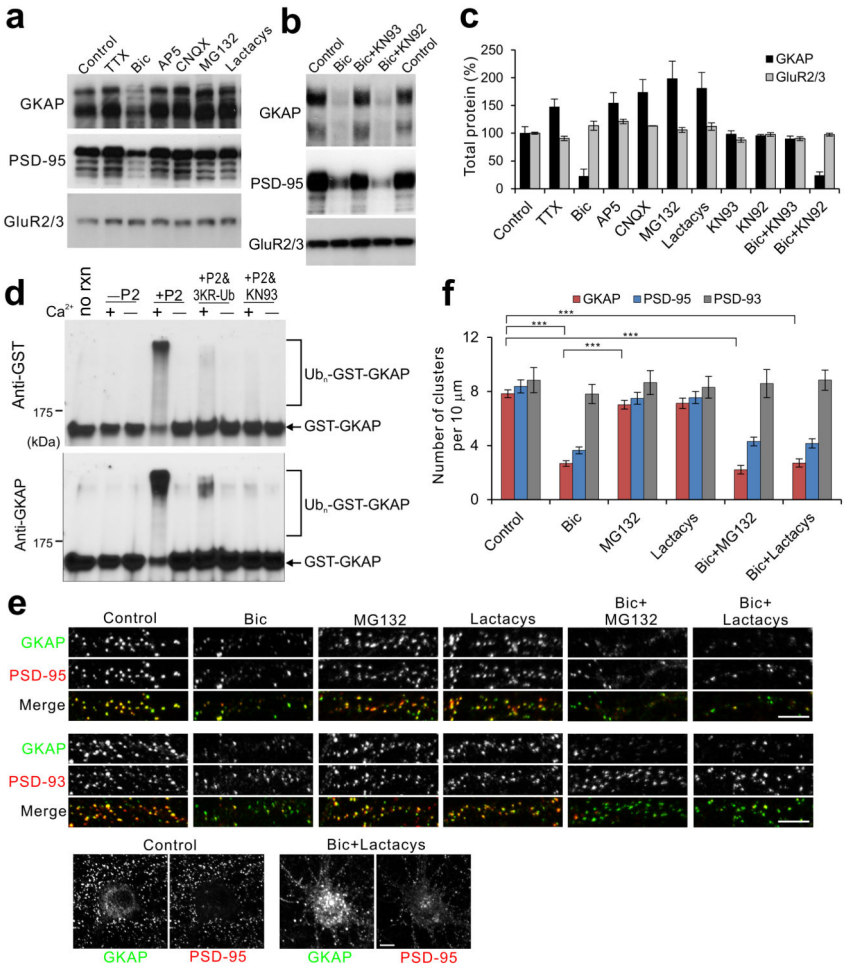

Figure 3.

CaMKII activity is required for the degradation of GKAP by the UPS. (**a,b**) Degradation of GKAP by activity modulation. Hippocampal culture neurons (18 DIV) were treated for 24 h with either DMSO (control), TTX (2 μM), Bic (40 μM), AP5 (100 μM), CNQX (50 μM), MG132 (50 μM), lactacystin (Lactacys, 10 μM), Bic + KN-93 (10 μM), or Bic + KN-92 (10 μM). Total protein extracts were prepared and examined for the indicated protein levels by Western blotting. Full-length blots are presented in Supplementary Figure 13. (**c**) Quantification of total protein level changes by the given treatments ($n = 3$). (**d**) *In vitro* ubiquitination of GKAP. Recombinant GST-GKAP (200 ng) was subject to in vitro ubiquitination reaction in the presence of either Ca^{2+} (+) or EGTA (–), and without (–P2) or with synaptosomal fraction (+P2) as a source of Ub-ligase and CaMKII. First lane represents GST-GKAP without the in vitro ubiquitination reaction (no rxn). In lanes 6 and 7, triple lysine Ub mutant (3KR-Ub) was substituted for Ub. In lanes 7 and 8, KN93 (10 μM) was added. After reaction, ubiquitination of GST-GKAP was determined by western blotting with anti-GST and anti-GKAP antibody. (**e**) Aggregate formation of GKAP after blocking proteasome activity. Neurons were treated with either Bic alone, MG132 alone, lactacystin alone, Bic + MG132, or Bic + lactacystin for 24 h, and examined for the localization of GKAP, PSD-95, and PSD-93 by immunocytochemistry. Bottom panels show the formation

of GKAP aggregates in the soma after Bic + MG132. (**f**) Quantification of cluster densities of GKAP, PSD-95, and PSD-93 24 h after the indicated treatments. $n \geq 25$ neurons per condition. *** $P < 0.001$. Scale bars, 5 μm. Error bars represent s.e.m.

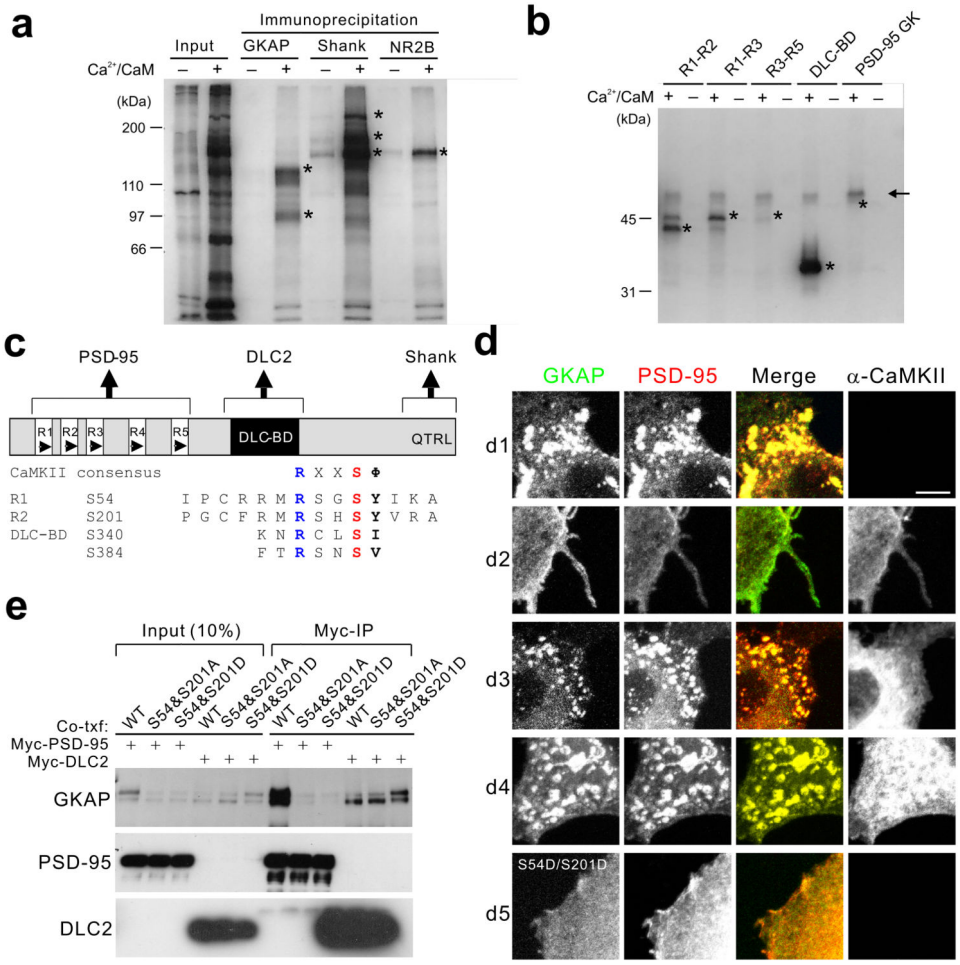

Figure 4.

Phosphorylation of GKAP by CaMKII prevents PSD-95 interaction. (**a**) Phosphorylation of GKAP, Shank, and NR2B by CaMKII in the PSDs. In situ phosphorylation reaction was performed with PSD I preparation (30 μg) and ^{32}P-γ-ATP in the presence of either Ca^{2+} (1 mM) and CaM (5 μM; + lanes) or EGTA (1 mM; –lanes). Phosphorylation of specific proteins was examined by immunoprecipitation with respective antibodies under denaturing condition and autoradiography. Input lanes show total protein phosphorylation profile. Asterisk (*) indicates the respective positions of immunoprecipitated proteins as determined by a parallel Western blotting. (**b**) In vitro phosphorylation of various domains of GKAP by purified CaMKII. Purified GST fusion proteins (100 ng) of GKAP comprising the various portions of GKAP were subject to in vitro phosphorylation reaction with purified rat brain CaMKII (10 ng) with or without Ca^{2+}/CaM (indicted by + or–, respectively). Protein phosphorylation is determined by SDS-PAGE and autoradiography. Asterisk (*) indicates the respective positions of proteins as determined by Coomassie blue staining. GST fusion protein of PSD-95 GK domain was used as a negative control. Arrow line indicates autophosphorylated CaMKII bands. (**c**) Domain structure of GKAP and conserved CaMKII phosphorylation sites. (**d**) Effects of α-CaMKII on co-cluster formation between GKAP and PSD-95. HA-GKAP and Myc-PSD-95 were co-transfected in COS cells and their

localization are examined by double immunofluorescence staining (green, GKAP; red, PSD-95). Co-transfected α-CaMKII is visualized by Cy-5 conjugated secondary antibodies (blue). Each panel shows a representative result from images taken from at least 20 cells per condition. Scale bars, 10 μm (**e**) Coimmunoprecipitation of GKAP and PSD-95 or DLC2 from COS cells. HA-tagged WT, phospho-defective (S54A/S201A), or phospho-mimic (S54D/S201D) GKAP was co-transfected into COS cells with either Myc-PSD-95 or Myc-DLC2 as indicated. After 24 h, total cell lysates were immunoprecipitated with anti-myc antibody (Myc-IP). Full-length blots are presented in Supplementary Figure 13.

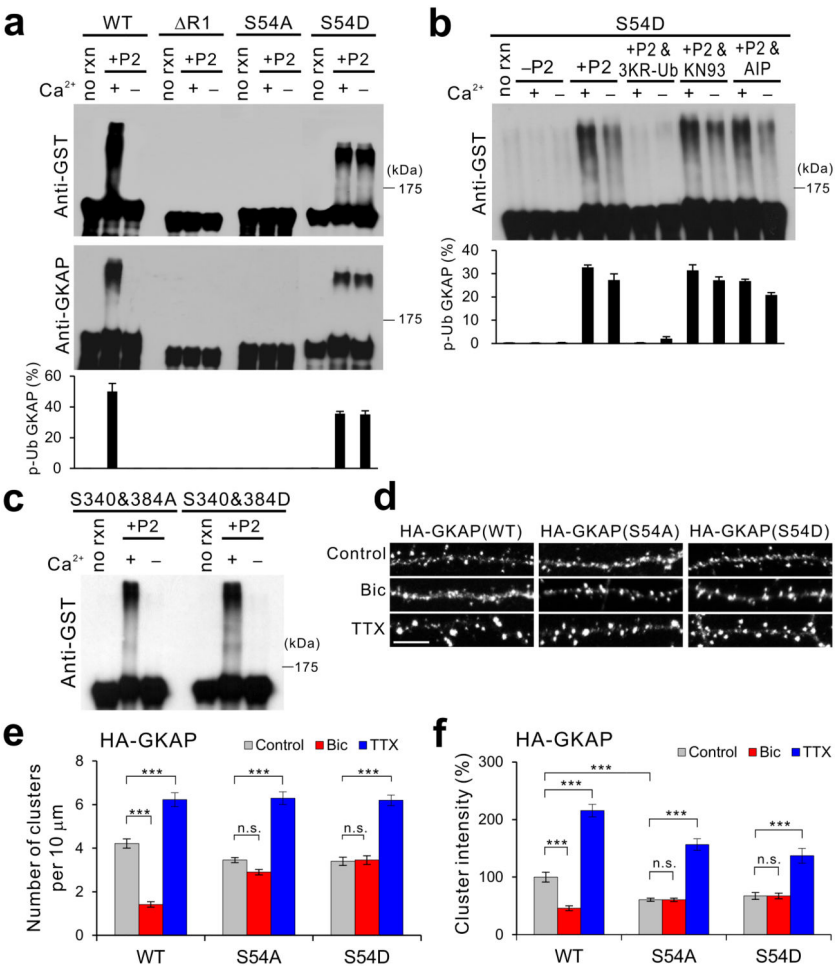

Figure 5.

Phosphorylation of Ser-54 in GKAP induces poly-ubiquitination and removal of GKAP from synapses. (**a**) *In vitro* ubiquitination of GST fusion proteins of GKAP WT, ΔR1, S54A, and S54D. Top two panels show representative results and quantification from triplicate experiments is shown at the bottom. Full-length blots are presented in Supplementary Figure 13. (**b**) Effect of Ca^{2+}, 3KR-Ub, and CaMKII inhibitors (KN93 and AIP) on the in vitro ubiquitination of S54D mutant. (**c**) Normal Ca^{2+}-dependent *in vitro* ubiquitination of GST fusion proteins of S340&384A and S340&384D mutants. (**d-f**) Activity-dependent turnover of S54A and S54D mutant in hippocampal neurons. Hippocampal neurons (14 DIV) were transfected with either HA-tagged WT, S54A, or S54D GKAP. Neurons were then treated with either Bic (40 μM) or TTX (2 μM) at 1 d post-transfection, and incubated further 36 h before fixation and immuno-staining for HA staining. (**d**) Representative images. Scale bar, 5 μm. (**e**) Quantification of HA cluster density. (**f**) Quantification of HA cluster intensity, normalized to WT control levels. $n > 20$ per condition. *** $P < 0.001$, ** $P < 0.01$, n.s., not significant. Error bars represent s.e.m.

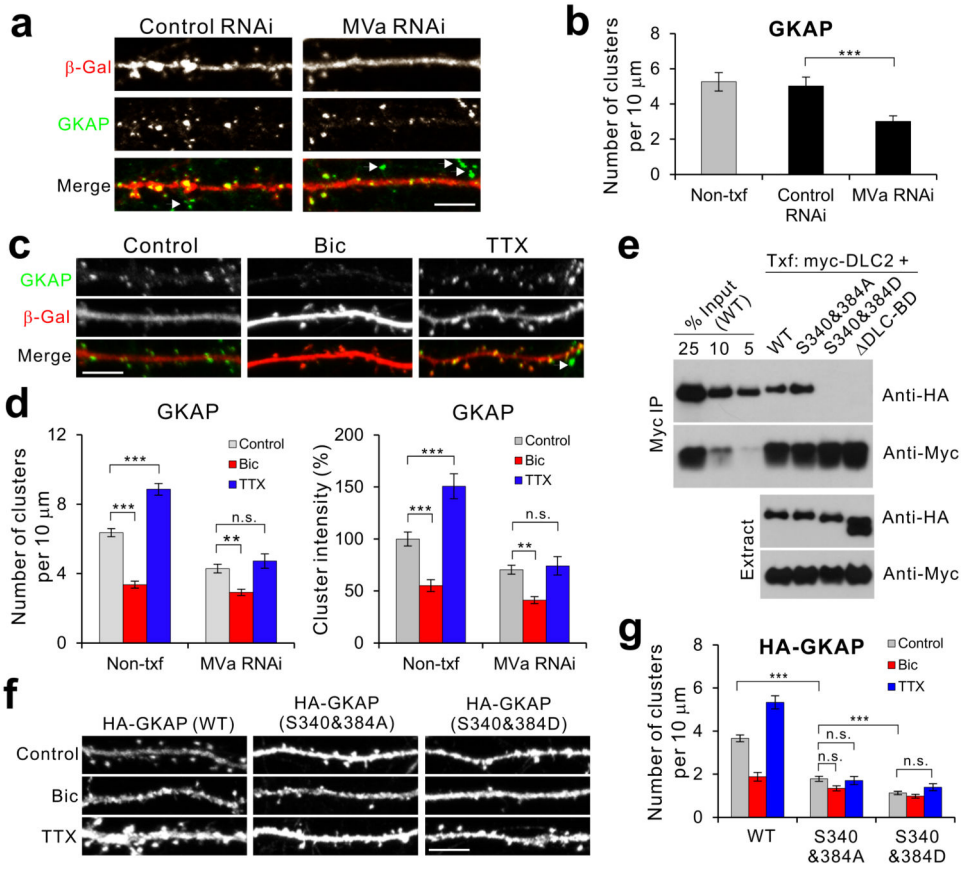

Figure 6.

Role of MyoVa-DLC and CaMKII phosphorylation in GKAP accumulation at synapses. (**a**) Effect of MyoVa (MVa) RNAi on synaptic GKAP accumulation. Cultured hippocampal neurons (14 DIV) were transfected with MVa RNAi and β-Gal, and examined for endogenous GKAP levels by immunofluorescent staining. (**b**) Quantification of GKAP cluster density after MVa RNAi. Control RNAi is Zn-T3 RNAi. *** $P < 0.001$. ($n = 20$ per group). Arrowheads in **a** and **b** indicate GKAP clusters from non-transfected neighboring neurons. (**c**) Effect of MVa RNAi on the activity-dependent changes in GKAP. (**d**) Quantification of activity-dependent changes of GKAP cluster density (left) and intensity (right) in MVa RNAi-transfected neurons. $n > 20$ per group. *** $P < 0.001$, ** $P < 0.01$, n.s., not significant. (**e**) Effect of CaMKII-phosphorylation site mutations in the DLC-binding domain of GKAP on the interaction of GKAP with DLC. Myc-DLC2 was co-transfected in COS cells with either HA-tagged WT, S340&384A, S340&384D, or ΔDLC-BD. DLC2 was immunoprecipitated with anti-myc antibody and the amounts of co-precipitating GKAP were determined by anti-HA blotting. Full-length blots are presented in Supplementary Figure 13. (**f**) Activity-dependent changes of GKAP phosphorylation mutants in the DLC-BD. Neurons were transfected with either HA-tagged WT, S340&384A, or S340&284D and treated with Bic or TTX for 36 h. Representative images (HA staining) of S340&384A and S340&284D mutant GKAP compared to WT. (**g**) Quantification of activity-dependent changes of S340&384A and S340&284D, measured by

HA staining. $n \geq 20$ neurons per condition. *** $P < 0.001$, ** $P < 0.01$. Scale bars, 5 μm. Error bars represent s.e.m.

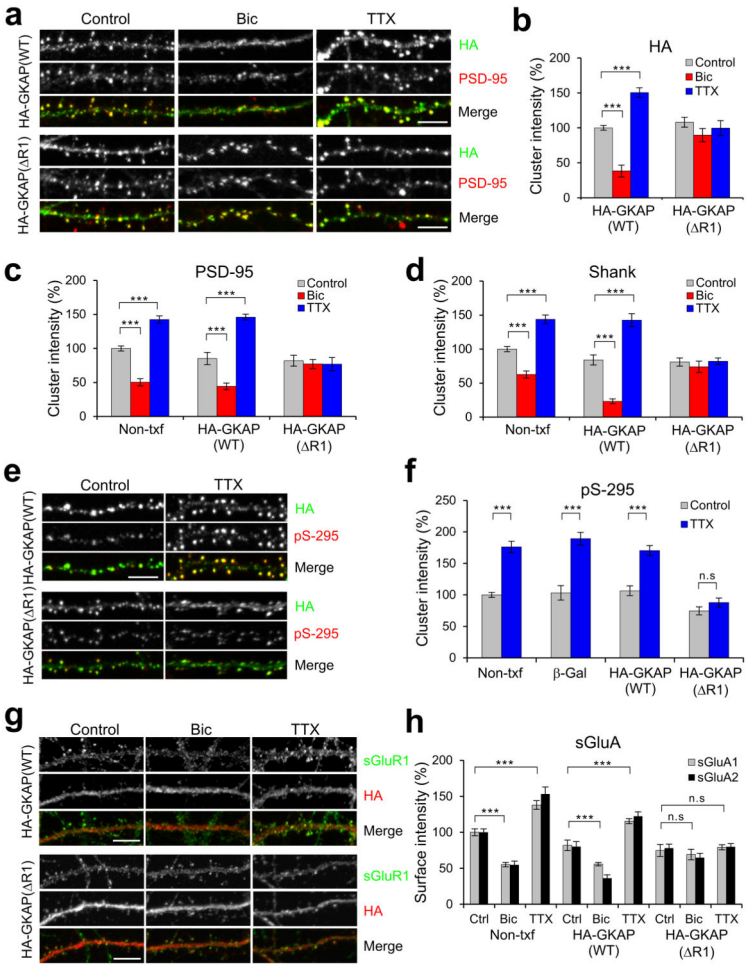

Figure 7.

GKAP (ΔR1) mutant blocks activity-dependent remodeling of PSD proteins. Hippocampal neurons (14 DIV) were transfected with HA-tagged WT or ΔR1 GKAP. After 1 d post-transfection, neurons were treated with either Bic (40 μM) or TTX (2 μM), and incubated further 24 h (for PSD-95 and Shank) or 48 h (for GluRs) before fixation and immuno-staining for the indicated proteins. (**a**) Effect of GKAP (WT) or GKAP (ΔR1) overexpression on the activity-dependent changes in endogenous PSD-95. (**b**) Quantification of activity-dependent changes of transfected WT or ΔR1 mutant GKAP, measured by HA cluster intensity (normalized to WT control level). $n > 20$ per condition. (**c,d**) Quantification of activity-dependent changes of endogenous PSD-95 (**c**) and Shank (**d**) in Non-txf, WT GKAP-, or ΔR1-transfected neurons. $n > 20$ per condition. (**e**) Effect of GKAP (WT) or GKAP (ΔR1) overexpression on the activity-dependent changes in the phosphorylation of Ser-295 (pS-295) of PSD-95. (**f**) Quantification of activity-dependent changes in the amount of pS-295 of PSD-95. $n \geq 20$ per condition. *** $P > 0.001$, n.s., not significant. (**g**) Effect of GKAP (WT) or GKAP (ΔR1) overexpression on the activity-dependent changes in surface expression of GluR1 (sGluR1). (**h**) Quantification of activity-dependent changes in surface expression of AMPA receptors. $n \geq 20$ per condition.*** $P > 0.001$, n.s., not significant. Scale bars, 5 μm. Error bars represent s.e.m.

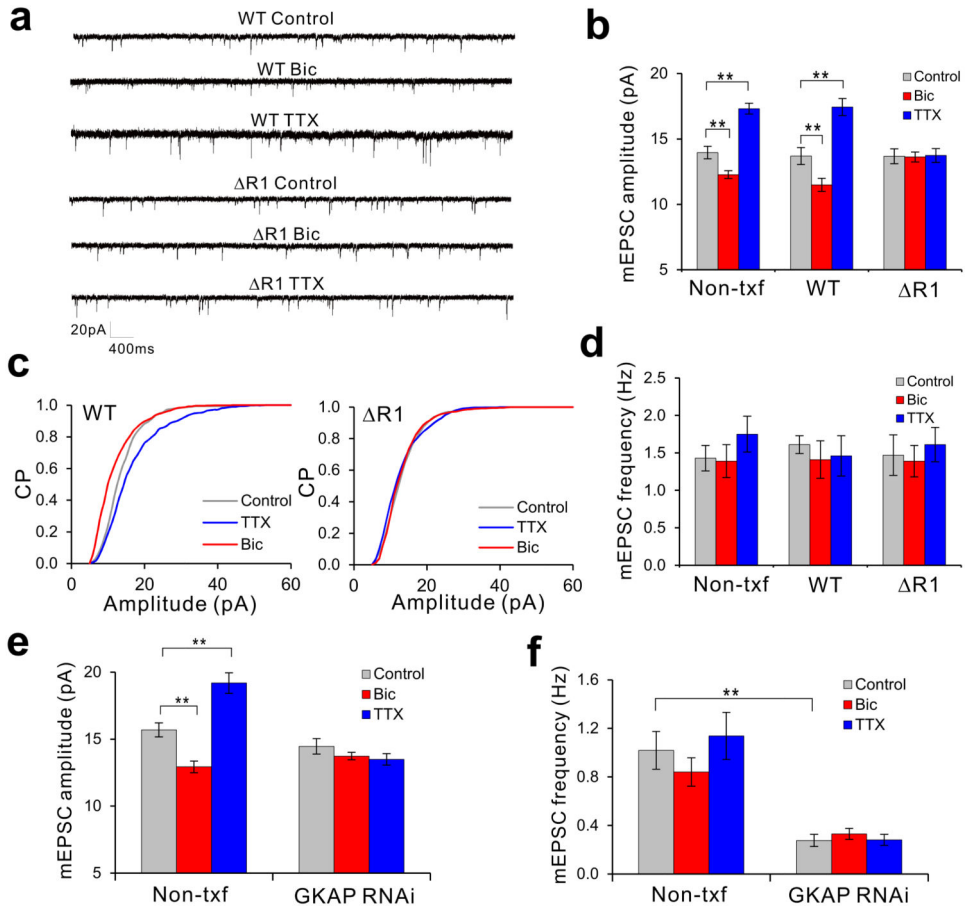

Figure 8.

GKAP turnover is critical for bi-directional homeostatic synaptic scaling. Hippocampal neurons (10 DIV) were transfected with HA-tagged WT or ΔR1 GKAP sub-cloned in pIRES2-EGFP. After 1 day post-transfection, neurons were treated with either Bic (40 μM) or TTX (2 μM), and incubated further 48 h before patch clamp recording. (**a**) Representative recording traces from hippocampal neurons transfected with GKAP WT or ΔR1 in control, TTX, and Bic condition. (**b**) Bar graphs showing average mEPSC amplitude of each group. ** $P < 0.01$ (t-test). $n > 12$ per condition. (**c**) Cumulative probability (CP) distribution of mEPSC amplitudes from all events in GKAP WT- and ΔR1–transfected neurons. WT; n = 1,486, 1,111, and 1,578 for control, Bic, and TTX, respectively. ΔR1; n = 1,276, 1,023, and 1,438 for control, Bic, and TTX, respectively. $P < 0.001$ (K-S test) for WT. (**d**) Bar graphs showing average mEPSC frequency of each group. (**e**) Effect of GKAP RNAi on average mEPSC amplitude. ** $P < 0.01$, $n > 15$ per condition. (**f**) Effect of GKAP RNAi on average mEPSC frequency. ** $P < 0.01$, $n > 15$ per condition. Error bars represent s.e.m.